Chemical Engineering Science 65 (2010) 651–659

Contents lists available at ScienceDirect

Chemical Engineering Science

journal homepage: www.elsevier.com/locate/ces

Continuous precipitation polymerization of vinylidene fluoride in supercritical carbon dioxide: A model for understanding the molecular-weight distribution

Tamer S. Ahmed [a], Joseph M. DeSimone [a,b], George W. Roberts [a,*]

[a] Department of Chemical and Biomolecular Engineering, North Carolina State University, Box # 7905, Raleigh, NC 27695-7905, USA
[b] Department of Chemistry, University of North Carolina at Chapel Hill, Box # 3290, Chapel Hill, NC 27599-3290, USA

ARTICLE INFO

Article history:
Received 23 January 2009
Accepted 26 August 2009
Available online 10 September 2009

Keywords:
Carbon dioxide
Supercritical fluid
Polymerization
Mathematical modeling
Bimodal molecular weight distribution
Model
Poly(vinylidene fluoride)

ABSTRACT

Poly(vinylidene fluoride) (PVDF) that is synthesized by precipitation polymerization in supercritical carbon dioxide ($scCO_2$) has a bimodal molecular weight distribution (MWD) and a very broad polydispersity index (PDI) under certain reaction conditions. Different models have been formulated to account for this behavior. This paper presents a homogenous model for a continuous stirred-tank reactor (CSTR) that includes the change of the termination reaction from kinetic control to diffusion control as the chain length of the polymeric radicals increases, and accounts for the change in the termination rate constant with macroradical chain length in the diffusion-controlled region. The model also includes the chain transfer to polymer reaction. Comparison of the model output with experimental data demonstrates that changes of the MWD, including the development of a bimodal distribution, with such reaction conditions as monomer concentration and average residence time are successfully predicted. In addition, the model can capture the occurrence of gelation, which appears to be responsible for a region of inoperability that was observed in the polymerization experiments. The success of this homogeneous model is consistent with recent research demonstrating that the CO_2-rich phase is the main locus of polymerization for the precipitation polymerization of vinylidene fluoride and vinylidene fluoride/hexafluoropropylene mixtures in $scCO_2$, at the conditions that have been studied to date.

1. Introduction

Poly(vinylidene fluoride) (PVDF) possesses unique properties such as excellent chemical, thermal and mechanical stability in addition to its pyroelectric and piezoelectric properties. Moreover, it has low surface energy, low water absorptivity, excellent weatherability and low flammability (Lovinger, 1982; Scheirs, 1997). Consequently, PVDF is used in applications requiring the highest purity, strength, and resistance to solvents, acids, bases, and heat, in addition to low smoke generation during a fire. Some typical applications for PVDF include coatings and films, cables, pipes, tubing in plastic heat exchangers, column packing, valves, and pumps. In addition, PVDF is an acceptable material for biological systems (Klinge et al., 2002).

The homopolymerization of vinylidene fluoride (VF2) in supercritical carbon dioxide ($scCO_2$) by both precipitation polymerization (Charpentier et al., 2000a, 1999; Galia et al., 2002; Liu et al., 2005; Mueller et al., 2005a; Saraf et al., 2002a, 2002b) and dispersion polymerization (Galia et al., 2006; Mueller et al., 2006; Tai et al., 2005a, 2005b, 2005c) has been reported in both continuous (Charpentier et al., 2000a, 1999; Saraf et al., 2002a, 2002b) and batch (Galia et al., 2002, 2006; Mueller et al., 2006; Tai et al., 2005a, 2005b, 2005c) reactors. The molecular weight distributions (MWDs) of the PVDF synthesized in $scCO_2$ exhibited bimodal distributions under certain reaction conditions, in both continuous (Saraf et al., 2002a, 2002b) and batch (Mueller et al., 2005a) operation. The main features associated with these bimodal MWDs (Saraf et al., 2002a) are: (1) the MWD changes from perfectly unimodal at low monomer concentrations to bimodal as the monomer concentration is increased at constant average residence time (τ), temperature and pressure; (2) the average residence time has no effect on the molecular weight and the MWD at low monomer concentration; (3) at high monomer concentrations, the polydispersity index (PDI) increases significantly with τ; and (4) the molecular weights, PDI, and the extent of bimodality decreases with increasing temperature.

High polydispersity indices and bimodality can contribute to better flow characteristics and processing behavior (Maccone et al., 2000; Tervoort et al., 2000). Therefore, the production of polymers with bimodal MWDs is potentially of commercial

* Corresponding author. Tel.: +1 919 515 7328; fax: +1 919 515 3465.
E-mail address: groberts@eos.ncsu.edu (G.W. Roberts).

0009-2509/$ - see front matter © 2009 Elsevier Ltd. All rights reserved.
doi:10.1016/j.ces.2009.08.039

interest. Typically, broad and bimodal MWDs are obtained by polymer blending, which usually requires a multi-step process where low and high molecular weight fractions are synthesized independently and then mixed together. On the other hand, polymerization in $scCO_2$ is a single step process. However, in order to synthesize polymer with the desired properties, it is very important to understand the origin of the bimodal MWD and broad PDI, and to be able to control the relative amounts and molecular weights of the two fractions.

Four different hypotheses have been proposed to explain the MWD of PVDF synthesized in $scCO_2$. The first is imperfect mixing in the continuous stirred tank reactor (CSTR) that was used in some polymerizations (Saraf et al., 2002a). This hypothesis was influenced by the work of Zhang and Ray (1997) in which it was shown that broad MWDs with a shoulder can be generated by imperfect mixing. However, experiments by Saraf et al., showed that changing the agitation rate and/or agitator type during the continuous precipitation polymerization of PVDF did not affect the MWD significantly (Saraf et al., 2002a).

The second hypothesis is that long chain branching, a result of chain transfer to polymer, caused a second population of highly branched chains (Saraf et al., 2002a). In order to explore this possibility, Saraf et al. developed a homogeneous kinetic model that included a chain transfer to polymer (CTP) reaction. This model, which was based on the assumption that all the reactions took place in the continuous phase, i.e., in the supercritical fluid, was successful in predicting the PDI variation with inlet monomer concentration and residence time. In addition, the model predicted a region of inoperability for the CSTR, coincided with experimental results. However, bimodal MWDs could not be generated with the model (Saraf et al., 2002a).

The third hypothesis is also based on the assumption that all the reactions took place in the supercritical fluid phase; bimodality is attributed to the transition of the termination reaction from a kinetically controlled regime to a diffusion-controlled regime with increasing macroradical molecular weight (Ahmed et al., 2004). Accordingly, the rate constant for termination decreases with chain length in the diffusion-controlled regime, and the second mode of the MWD is a result of an increased population of high-molecular-weight macroradicals. In fact, the decrease in termination rate constant with radical chain length was previously reported to produce bimodal MWDs for the free-radical polymerization of methyl methacrylate in the presence of poly(methyl methacrylate) (Bogunjoko and Brooks, 1983).

In order to explore the third hypothesis, we previously proposed a homogeneous kinetic model for VF2 polymerization in a CSTR incorporating a termination rate constant that decreased with macroradical-chain-length for long chains (Ahmed et al., 2004). In this model, three termination reactions with different rate constants were used to approximate the actual termination scheme consisting of an infinite number of reactions and rate constants. The model captured the directional effect of the operating parameters, such as monomer feed concentration, residence time, and reaction temperature, on the MWD. However, the model seriously underestimated the PDIs that were observed in some experiments, and did not predict a region of inoperability. Presumably, these deficiencies resulted from ignoring the CTP reaction.

The fourth and final hypothesis is that bimodality results from simultaneous polymerization in both the supercritical fluid and the polymer phases (Mueller et al., 2005a; Saraf et al., 2002a, 2002b). Mueller et al. developed a mathematical model for the dispersion polymerization of poly(methyl methacrylate) in $scCO_2$ that accounted for simultaneous polymerization in both phases by taking into account the transport of polymeric radicals between the two phases (Mueller et al., 2004, 2005b). They then applied this model to the precipitation polymerization of PVDF in $scCO_2$ (Mueller et al., 2005a).

The "simultaneous polymerization" model included a large number of parameters. Mueller et al. made a considerable effort to estimate most of these parameters from independent sources. Nevertheless, three parameters had to be adjusted to model VF2 polymerization; two of these parameters had a very significant impact on the existence or the non-existence of a bimodal MWD (Mueller et al., 2005a). Mueller et al. compared the model predictions to batch polymerization data for PVDF and found reasonable agreement. That work establishes that the simultaneous polymerization in both the supercritical phase and the polymer particles can lead to bimodal molecular weight distributions. However, it does not establish that "simultaneous polymerization" is the cause of, or even a major contributor to, the bimodal MWDs that were observed for VF2 polymerization in $scCO_2$.

For precipitation/dispersion polymerization, two factors determine the importance of polymerization in the polymer phase relative to that in the fluid phase: (1) the time scale of the termination reaction compared to that of macroradical precipitation and/or transport between phases; and (2) the concentration of monomer dissolved in the polymer phase. Regarding the first factor, if the characteristic time for termination is much less than that for precipitation/transport, the polymer chains will terminate in the fluid phase before macroradicals transfer to the polymer phase and vice versa. Mueller et al. (2005a) introduced the Ω-parameter, i.e., the ratio of the characteristic time for interphase mass transport of radicals to that for termination, to quantify this relationship. They neglected the precipitation of macroradicals, which may be a more important means of radical transfer to the polymer phase, especially for long chain lengths. For precipitation polymerization of PVDF, the estimated values of Ω in the polymer phase were negligible, $\ll 1$, while the Ω parameter for the continuous phase was smaller than one, except for macroradicals with a very high degree of polymerization, where Ω values very close to one were obtained. These predictions suggest that both the polymer and fluid phases are possible loci of polymerization, at the conditions of the experiments. It is important to recognize that these values for the Ω-parameter depend on the specific interphase surface area of the polymer particles. This is one of the key adjustable parameters in the Mueller et al. (2005a) model, and has a significant impact on the model output. Small changes in the value of the total area of the particles are sufficient to completely change the MWD predicted by the model (Mueller et al., 2005a).

The second factor that has a significant impact on polymerization behavior is the solubility of VF2 in the polymer phase at reaction conditions. Recently, the simultaneous equilibrium sorption of CO_2 and VF2 into PVDF has been studied experimentally by Galia et al. (2008). They showed that the concentration of VF2 in the polymer particles is very low at the conditions used during the polymerization of VF2 in $scCO_2$. These results coincide with a similar study by our research group showing that the equilibrium partition coefficient of VF2 between PVDF and CO_2 is negligible at high pressures (Kennedy, 2003; Saraf et al., 2002b). The limited solubility of VF2 in PVDF in the presence of $scCO_2$ suggests that any radical initiated or captured in the polymer phase propagates under monomer-starved conditions that could compensate the autoacceleration effect arising from the impeded termination in the polymer phase (Galia et al., 2008), and lead to a very low rate of polymerization in the polymer phase.

Mueller et al. (2005a) used the Sanchez–Lacombe equation of state with the mixing rules proposed by McHugh and Krukonis (1994) to describe the partitioning of VF2 between the fluid and polymer phases. Experimental data (Kennedy, 2003) were used to

obtain the interaction coefficients of VF2/CO_2 and CO_2/PVDF. For VF2/PVDF, Mueller et al. neglected the entropic interaction parameter and used the other binary interaction parameter as an adjustable parameter. Unfortunately, their method of adjusting this parameter to fit the experimental data was not described. However, the values of the VF2/PVDF interaction coefficients used in the Sanchez–Lacombe equation of state by Mueller et al. were different from values reported by Galia et al. (2008) by fitting their experimental sorption data.

A final concern about the use of the "simultaneous polymerization" hypothesis to account for the bimodal MWDs and high PDIs observed for PVDF rests in a recent study (Ahmed et al., 2009), which established that the precipitation homopolymerization of VF2 and the precipitation copolymerization of VF2 with hexafluoropropylene in $scCO_2$ takes place primarily in the continuous, CO_2-rich fluid phase, at the conditions that have been studied experimentally. Analysis of experimental data has shown that the measured rate of polymerization (R_p) and number-average molecular weight (M_n) are well described by a model based on the assumption that all of the polymerization reactions take place in the fluid phase. Conversely, two models based on the assumption that propagation and termination take place either on the surface of the polymer particles or throughout the polymer particles fail to describe the R_p and M_n data. On other hand, an approximate deconvolution of the bimodal MWDs obtained by Saraf et al. (2002a) for experiments at VF2 inlet concentrations of 2.8 and 3.5 mol/L showed that approximately 60–70% of the monomer units are in the second, high molecular weight peak (Ahmed et al., 2009). According to the "simultaneous polymerization" model, this fraction of the monomers reacted would have been polymerized in the polymer phase. This is clearly inconsistent with the observed kinetics of VF2 polymerization (Ahmed et al., 2009).

The objective of the current work is to demonstrate that a homogenous model that accounts for both the CTP reaction and the chain-length dependency of the termination rate constant can capture all the important features of the MWDs of PVDF prepared by continuous precipitation polymerization in $scCO_2$. The experimental data for the precipitation polymerization of PVDF in $scCO_2$ using a CSTR at 75 °C and 276 bar with diethylperoxydicarbonate (DEPDC) initiator reported by Saraf et al. (2002a) are used to test the performance of the model.

2. Modeling

2.1. Model development

The model is based on the reactions shown in Fig. 1. The first three steps are classical: initiator decomposition, chain initiation, and chain propagation. Termination is solely by combination (Saraf et al., 2002a) and is represented by three separate reactions

$$I \xrightarrow{k_d} 2f\ R^{\bullet} \quad \text{(Initiator decomposition)}$$
$$R^{\bullet} + M \xrightarrow{k_{in}} R_1^{\bullet} \quad \text{(Chain Initiation)}$$
$$R_n^{\bullet} + M \xrightarrow{k_p} R_{n+1}^{\bullet} \quad \text{(Propagation)}$$
$$R_n^{\bullet} + R_m^{\bullet} \xrightarrow{k_t^{uu}} P_{n+m} \quad (\text{Termination}, n \,\&\, m \le n_{cr})$$
$$R_n^{\bullet} + R_m^{\bullet h} \xrightarrow{k_t^{uh}} P_{n+m} \quad (\text{Termination}, n \le n_{cr} \,\&\, m > n_{cr})$$
$$R_n^{\bullet h} + R_m^{\bullet h} \xrightarrow{k_t^{hh}} P_{n+m} \quad (\text{Termination}, n \,\&\, m > n_{cr})$$
$$P_n + R_m^{\bullet} / R_m^{\bullet h} \xrightarrow{nk_{tr}} P_n^{\bullet} + P_m \quad \text{(Chain transfer to polymer)}$$

Fig. 1. Proposed kinetic scheme for PVDF polymerization in $scCO_2$. I, M, $R_n^{\bullet}$, $R_n^{\bullet h}$ and P_n denote initiator, monomer, unhindered radicals, hindered radicals and dead polymer, respectively.

between macroradicals of different chain lengths. This is perhaps the simplest approximation that permits the termination rate constant to be a function of macroradical chain length. When both radicals are shorter than some critical chain length, n_{cr}, the termination reaction is assumed to be kinetically controlled and the termination rate constant, k_t^{uu}, is not chain-length dependent. When either or both of the macroradicals contains more than n_{cr} monomer units, the termination reaction becomes diffusion controlled and the termination rate constant is chain length-dependent. Radicals containing up to n_{cr} monomer units are referred to as unhindered, while hindered radicals are those containing more than n_{cr} units. For radicals of chain length greater than the critical value, the reduction in the termination rate due to the diffusion limitations is approximated by two termination rate constants (k_t^{uh}) and (k_t^{hh}). The rate constant k_t^{uh} describes termination by combination of an unhindered radical with a hindered radical. The rate constant k_t^{hh} describes the combination of two hindered radicals. This scheme is similar to the one used by Bogunjoko and Brooks (1983). It is a major simplification of the actual chemistry, in that an infinite number of reactions and rate constants are lumped into three groups by creating two groups of macroradicals. Even with this simplification, the mathematics required to solve for the MWD is tedious. The simplest extension of this lumping approach would be to create three groups of macroradicals, which leads to six termination reactions and rate constants.

As an addition to our previous model (Ahmed et al., 2004), the CTP reaction was taken into account. No diffusion limitations are expected for radical propagation or CTP reactions or since these reactions are slow compared to termination reactions (Odian, 2004).

The model is derived for polymerization in an ideal CSTR operating at steady state with the following main assumptions and characteristics:

(1) The continuous CO_2 phase is the only locus of polymerization (i.e. the rates of any reaction occurring in the polymer phase are negligible compared to the rates in the fluid phase).
(2) The quasi-steady-state approximation is valid. This assumption implies that the lifetime of radicals is very small compared to the average residence time of the CSTR. Hence, the radical outflow from the CSTR is neglected.
(3) In the CTP step, a hydrogen atom is extracted from any one of the repeat units of the dead polymer. Therefore, the rate constant is proportional to the chain length of the "dead" polymer molecule. Shielding of the inner portion of the molecules, which is possible in the case of large, coiled molecules, is neglected.

2.2. Model equations

Let $R_n^{\bullet}$ and $R_n^{\bullet h}$ be the concentrations of the unhindered ($n \le n_{cr}$) and hindered ($n > n_{cr}$) radicals containing n monomer units, respectively. The steady-state material balances on live polymers give

$$R_1^{\bullet} = \frac{2fk_dI}{k_pM}\Delta \tag{1}$$

$$R_n^{\bullet} = \Delta[R_{n-1}^{\bullet} + nP_n\Phi],\ 1 < n \le n_{cr} \tag{2}$$

$$R_n^{\bullet h} = \Psi[R_{n-1}^{\bullet h} + nP_n\Phi],\ n > n_{cr} \tag{3}$$

where

$$(R_n^{\bullet})_T = \sum_{n=1}^{n_{cr}} R_n^{\bullet} \tag{4}$$

$$(R_n^{\bullet h})_T = \sum_{n=n_{cr}+1}^{\infty} R_n^{\bullet h} \tag{5}$$

$$\Phi = \frac{k_{tp}((R_n^{\bullet})_T + (R_n^{\bullet h})_T)}{k_p M} \tag{6}$$

$$\Delta = \frac{k_p M}{k_p M + 2k_t^{uu}(R_n^{\bullet})_T + 2k_t^{uh}(R_n^{\bullet h})_T + k_{tp}\sum_{n=2}^{\infty} nP_n} \tag{7}$$

$$\Psi = \frac{k_p M}{k_p M + 2k_t^{uh}(R_n^{\bullet})_T + 2k_t^{hh}(R_n^{\bullet h})_T + k_{tp}\sum_{n=2}^{\infty} nP_n} \tag{8}$$

Eq. (2) can be written as a finite sum of terms in P_n by using the expression for $R_1^{\bullet}$ given by Eq. (1):

$$R_n^{\bullet} = \left(\frac{2fk_dI}{k_pM}\right)\Delta^n + \Phi\sum_{m=1}^{n-1}(\Delta^{n-m}(m+1)P_{m+1}), 1 < n \le n_{cr} \tag{9}$$

Similarly, Eq. (3) can be rewritten in terms of $R_{n_{cr}}^{\bullet}$:

$$R_n^{\bullet h} = \Psi^{n-n_{cr}}R_{n_{cr}}^{\bullet} + \Phi\sum_{m=n_{cr}}^{n-1}(\Psi^{n-m}(m+1)P_{m+1}), n > n_{cr} \tag{10}$$

where $R_{n_{cr}}^{\bullet}$ is obtained from Eq. (9) by setting $n=n_{cr}$:

$$R_{n_{cr}}^{\bullet} = \left(\frac{2fk_dI}{k_pM}\right)\Delta^{n_{cr}} + \Phi\sum_{m=1}^{n_{cr}-1}(\Psi^{n_{cr}-m}(m+1)P_{m+1}) \tag{11}$$

Substituting Eq. (9) into Eq. (4) gives the total concentration of unhindered radicals:

$$(R_n^{\bullet})_T = \left(\frac{2fk_dI}{k_pM}\right)\sum_{n=1}^{n_{cr}}\Delta^n + \Phi\sum_{n=2}^{n_{cr}}\sum_{m=1}^{n-1}(\Delta^{n-m}(m+1)P_{m+1}) \tag{12}$$

The total concentration of hindered radicals is obtained by substituting Eqs. (10) and (11) into Eq. (5)

$$\begin{aligned}(R_n^{\bullet h})_T = {} & \left(\frac{2fk_dI}{k_pM}\right)\left(\frac{\Delta}{\Psi}\right)^{n_{cr}}\sum_{n=n_{cr}+1}^{\infty}\Psi^n \\ & + \Phi\sum_{n=n_{cr}+1}^{\infty}\left\{\Psi^{n-n_{cr}}\sum_{m=1}^{n_{cr}-1}(\Psi^{n_{cr}-m}(m+1)P_{m+1})\right. \\ & \left. + \sum_{m=n_{cr}}^{n-1}(\Psi^{n-m}(m+1)P_{m+1})\right\}\end{aligned} \tag{13}$$

Since $\Delta < 1$ and $\Psi < 1$, use of the binomial series reduces Eqs. (12) and (13) to

$$(R_n^{\bullet})_T = \left(\frac{2fk_dI}{k_pM}\right)\frac{\Delta}{1-\Delta}(1-\Delta^{n_{cr}}) + \Phi\sum_{n=2}^{n_{cr}}\sum_{m=1}^{n-1}(\Delta^{n-m}(m+1)P_{m+1}) \tag{14}$$

$$\begin{aligned}(R_n^{\bullet h})_T = {} & \left(\frac{2fk_dI}{k_pM}\right)\Delta^{n_{cr}}\left(\frac{\Psi}{1-\Psi}\right) \\ & + \Phi\sum_{n=n_{cr}+1}^{\infty}\left\{\Psi^{n-n_{cr}}\sum_{m=1}^{n_{cr}-1}(\Psi^{n_{cr}-m}(m+1)P_{m+1})\right. \\ & \left. + \sum_{m=n_{cr}}^{n-1}(\Psi^{n-m}(m+1)P_{m+1})\right\}\end{aligned} \tag{15}$$

A steady state material balance on dead polymer gives

$$P_n = \tau\left\{k_t^{uu}\sum_{m=1}^{n-1}(R_m^{\bullet}R_{n-m}^{\bullet}) + k_{tp}\left[R_n^{\bullet}\sum_{m=2}^{\infty}(mP_m) - nP_n((R_n^{\bullet})_T + (R_n^{\bullet h})_T)\right]\right\}, \quad 1 < n \le n_{cr} \tag{16}$$

$$P_n = \tau(r_{p_n}^a + r_{p_n}^b + r_{p_n}^c + r_{p_n}^d), n > n_{cr} \tag{17}$$

where τ is the average residence time:

$$\tau = \frac{\text{Volume of CSTR}}{\text{Total volumetric flow rate}}$$

$$r_{p_n}^a = \left\{\begin{array}{ll} k_t^{uu}\sum_{m=n-n_{cr}}^{n_{cr}}(R_m^{\bullet}R_{n-m}^{\bullet}), & n_{cr} < n \le 2n_{cr} \\ 0, & n > 2n_{cr}\end{array}\right\} \tag{18}$$

$$r_{p_n}^b = \left\{\begin{array}{ll} 2k_t^{uh}\sum_{m=1}^{n-(n_{cr}+1)}(R_m^{\bullet}R_{n-m}^{\bullet h}), & n_{cr}+1 < n \le 2n_{cr}+1 \\ 2k_t^{uh}\sum_{m=1}^{n_{cr}}(R_m^{\bullet}R_{n-m}^{\bullet h}), & n > 2n_{cr}+1\end{array}\right\} \tag{19}$$

$$r_{p_n}^c = \left\{\begin{array}{ll} 0, & n_{cr} < n < 2n_{cr}+2 \\ k_t^{hh}\sum_{m=n_{cr}+1}^{n-(n_{cr}+1)}(R_m^{\bullet h}R_{n-m}^{\bullet h}), & n \ge 2n_{cr}+2\end{array}\right\} \tag{20}$$

$$r_{p_n}^d = k_{tp}[R_n^{\bullet h}\sum_{2}^{\infty}(mP_m) - nP_n((R_n^{\bullet})_T + (R_n^{\bullet h})_T)], n > n_{cr} \tag{21}$$

Finally, steady-state material balances on monomer and initiator give

$$M = \frac{M_{in} - 2fk_dI\tau}{1 + \tau k_p((R_n^{\bullet})_T + (R_n^{\bullet h})_T)} \tag{22}$$

$$I = \frac{I_{in}}{1 + k_d\tau} \tag{23}$$

where M_{in} and I_{in} are the feed concentrations of monomer and initiator, respectively, and f and k_d are the initiator decomposition efficiency and decomposition rate constant, respectively.

These equations permit the performance of a CSTR operating at a known set of conditions (T, P, τ, M_{in}, I_{in}) to be calculated. The algorithm used to perform these calculations is outlined in the Supplementary data. To perform these calculations, eight parameters must be known: k_d, f, k_p, k_{tp}, n_{cr}, k_t^{uu}, k_t^{uh}, and k_t^{hh}.

2.3. Parameter determination

2.3.1. Initiator decomposition

The decomposition kinetics of DEPDC in $scCO_2$ was studied by Charpentier et al. (2000b). Their values, at 75 °C, f=0.6 and $k_d = 9.9\times10^{-4}\,s^{-1}$, were used here.

2.3.2. Critical chain length

The model predicts that the location of the minimum between the two peaks of a bimodal MWD is located at a chain length of $2n_{cr}+1$. Therefore, the value of n_{cr} can be estimated from the experimental MWDs. Experimentally, the location of this minimum increases slightly as the monomer concentration increases (Saraf et al., 2002a). However, for the sake of simplicity, a constant value of 540 was used for MWDs at 75 °C.

2.3.3. Termination rate constants

The Russell (1994, 1995) model was used to describe the chain-length-dependence of the termination rate constant. Neglecting reaction diffusion, which is important only at very high conversions, the dependence of the termination rate constant $k_t(i,j)$ on chain length is given by

$$k_t(i,j) = 2\pi p_{spin}(D_i + D_j)\sigma N_A \tag{24}$$

$$D_i = \left\{\begin{array}{ll} D_{mon}/i^a, & i \le X_c \\ D_{mon}(X_c)^{b-a}/i^b, & i > X_c\end{array}\right\} \tag{25}$$

Here N_A is Avogadro's number; σ is the capture radius of the reaction (a value of 0.3 nm (Benson and North, 1959; Mahabadi and O'Driscoll, 1977), typical for vinyl–vinyl combination, was used here); p_{spin} is the spin probability (since $scCO_2$ at the reaction conditions (276 bar and 75 °C) has a liquid-like density, a value of 0.25 was chosen (Russell, 1995)); D_i is the diffusion coefficient of the growing chains; D_{mon} is the diffusion coefficient of the monomer (a value of 1.4×10^{-8} m^2/s at 75 °C and 276 bar was estimated for the diffusivity of vinylidene fluoride monomer in $scCO_2$ using the method proposed by Riazi and Whitson (1993)); X_c is the crossover chain length at which the scaling law changes from short- to long-chain diffusion, while a and b are the chain-length exponents (typical values lie in the range 0.5–0.6 for dilute conditions (de Kock et al., 2001)).

The termination rate constants were estimated by using the functional form of the chain dependence given by Eqs. (24) and (25), but without a crossover chain length X_c (Buback and Kuchta, 1997; Deady et al., 1993). A single average chain-length exponent of 0.55 was used. Weighted-average chain lengths of 285 and 39,000 monomer units were used to represent the average unhindered and hindered radical, respectively, at 75 °C. These values were obtained by a trial-and-error procedure. Using assumed values, the three termination rate constants were calculated as described above. The model code then was executed using the parameters from a single experimental point (M_{in}=3.5 M, I_{in}=0.003 M, τ=21 min, 75 °C, 276 bar) to obtain the complete radical distribution. From the radical distribution, weighted-average chain lengths were calculated and were compared to the assumed ones. If necessary, the assumed values were adjusted and the procedure was repeated.

There is no published value for the kinetic-controlled termination rate constant for the current system. Consequently, the value of k_t^{uu} used in the model was chosen to be less than the corresponding value of the diffusion-controlled termination rate constant between unhindered radicals calculated from Russell model (the value used is: $k_t^{uu}=3.47\times10^8$ L/mol s). The value of k_t^{uu} has only a minor effect on the first mode in the MWD and essentially no effect on the overall performance of the model. As for the other two termination rate constants, the values obtained from the Russell model were: $2k_t^{uh}=1.91\times10^8$ L/mol s, and $k_t^{hh}=2.4\times10^7$ L/mol s.

2.3.4. Propagation rate constant

The value of k_p was calculated from the reported values for $k_p/\langle k_t\rangle^{0.5}$ for the precipitation polymerization of PVDF in $scCO_2$ at 75 °C and 276 bar (Charpentier et al., 2000a), where $\langle k_t\rangle$ (the average macroscopic termination rate constant) was approximated from Eq. (26). A value of k_p=2775 L/mol s was obtained

$$\langle k_t\rangle=\frac{\sum_i\sum_j k_t(i,j)R_i^{\bullet}R_j^{\bullet}}{(\sum_i R_i^{\bullet})^2}\approx\frac{k_t^{uu}\sum_{i=1}^{n_{cr}}\sum_{j=1}^{n_{cr}}R_i^{\bullet}R_j^{\bullet}+2k_t^{uh}\sum_{i=1}^{n_{cr}}\sum_{j=n_{cr}+1}^{\infty}R_i^{\bullet}R_j^{\bullet h}+k_t^{hh}\sum_{i=n_{cr}+1}^{\infty}\sum_{j=n_{cr}+1}^{\infty}R_i^{\bullet h}R_j^{\bullet h}}{[(R_n^{\bullet})_T+(R_n^{\bullet h})_T]^2} \tag{26}$$

2.3.5. Chain transfer to polymer rate constant

The rate constant for the CTP reaction was estimated by fitting the experimental PDI at M_{in}=3.5 M, I_{in}=0.003 M, τ=21 min, 75 °C, 276 bar. A value of $k_{tp}/k_p=1.5\times10^{-3}$ was obtained.

3. Results and discussion

Fig. 2 shows the experimental MWDs (Saraf et al., 2002a) along with the model predictions for a series of experiments with monomer feed concentration varying from 0.77 to 3.5 M at otherwise constant conditions. The model predicts the change from a unimodal to a bimodal MWD very well. For the lowest monomer concentration (0.77 M), the predicted MWD is perfectly unimodal with a PDI of 1.5. As monomer concentration increases to 1.7 M, the model predicts a slight inflection (shoulder) in the MWD. This inflection is evident in the experimental MWD curve. Finally, for the two highest monomer concentrations, the predicted MWDs are bimodal, which coincides with the experimental results.

The model captures many important features of the experimental data. Specifically, as the feed monomer concentration increases: (1) the MWD changes from perfectly unimodal to bimodal; (2) the area of the high-molecular-weight peak increases relative to the area of the low-molecular-weight peak; (3) both peaks shift to higher molecular weights; and (4) a long, high-molecular-weight tail appears for the highest feed monomer concentration (3.5 M). However, the model tends to underpredict the location of the molecular-weight peaks of the polymer at all four inlet monomer concentrations. This issue will be discussed later in the paper

Fig. 3 compares the model predictions for the PDI with the experimental PDIs (Saraf et al., 2002a) at the various feed monomer concentrations. The inclusion of the CTP reaction allows the model to predict the experimental PDI, and its trend with monomer concentration, reasonably well. In particular, the abrupt increase in the PDI near the highest monomer concentration is captured by the model. Note, however, that the data point at the highest concentration was the one that was used to determine some of the unknown kinetic parameters, including k_{tp}.

Figs. 4 and 5 show the predicted effect of τ on the MWDs for low and high monomer feed concentrations, respectively, along with the corresponding experimental MWDs (Saraf et al., 2002a). Essentially identical unimodal MWDs are predicted with increasing τ for the low monomer concentration (0.78 M). This behavior matches that of the experimental MWDs. At the high monomer concentration (2.8 M), the current model provides a much better prediction for the experimental MWDs than the original model without CTP (Ahmed et al., 2004). In particular, the model captures the very long, high-molecular-weight tail that appeared for the polymer produced at 25.5 min residence time. This experiment was not used to evaluate any of the parameters in the model.

Predictions for the effect of τ on the PDI for low and high monomer concentrations are shown in Fig. 6. For the low monomer concentration (0.78 M), the model predicts that the PDI is close to 1.5 over the whole range of residence times, in agreement with the experimental values. At the high monomer concentration (2.8 M), the model overestimates the PDI to some extent. Nevertheless, the trend of the PDI, and particularly its abrupt increase at higher residence times, is captured adequately.

The sharp increase in the PDI at higher residence times that was observed experimentally and is shown in Figs. 3 and 6 is believed to be caused by crosslinking resulting from the CTP reaction plus termination by combination. During the polymerization experiments, a region of inoperability was observed, where the CSTR could not be brought to steady state (Saraf et al., 2002a). This inoperability region was associated with long residence times and high inlet monomer concentrations, and was attributed to gelation in the continuous phase due to polymer

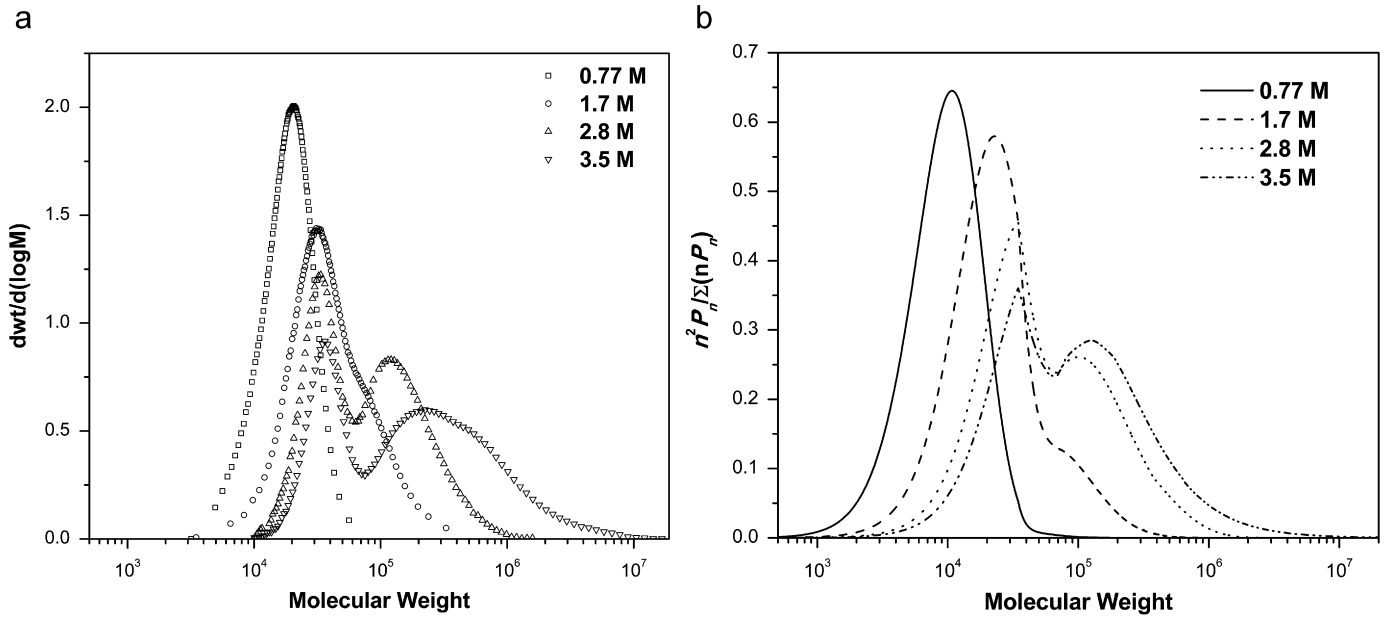

Fig. 2. Effect of monomer feed concentration on MWD: (a) experimental (Saraf et al., 2002a); (b) model: the *y*-axis is proportional to the experimental one. 75 °C, 276 bar, I_{in}=0.03 M, and 21 min average residence time.

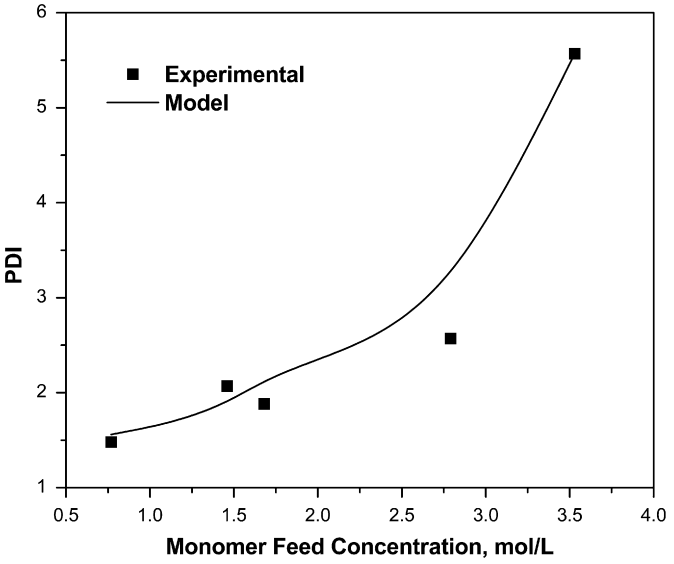

Fig. 3. Effect of monomer feed concentration on PDI. 75 °C, 276 bar, I_{in}=0.03 M, and 21 min average residence time.

crosslinking (Dotson et al., 1996; Odian, 2004; Tobita, 1993). The ability of the model to predict a steep increase in the PDI for both high monomer concentrations (Fig. 3) and high residence times (Fig. 6) suggests its ability to capture the inoperability region that was observed (Saraf et al., 2002a). However, no attempt was made to predict the boundaries of the region with the present model.

Naturally, the predicted PDI is sensitive to the assumed value of k_{tp}. The value of (k_{tp}/k_p) used in this study at 75 °C (k_{tp}/k_p= 1.5×10^{-3} with k_p=2775 L/mol s) is three orders of magnitude higher than the value used by Mueller et al. (2005a) in their "simultaneous polymerization" model of VF2 polymerization ($k_{tp}/k_p=1\times10^{-6}$ with k_p=3870 L/mol s), at a somewhat lower temperature (50 °C), and is at the upper end of the range of values (10^{-6}–10^{-3}) provided in the literature (Odian, 2004). The capture of the above-mentioned mechanism of crosslinking in the Mueller et al. (2005a) model is uncertain in view of their very low value of the CTP rate constant. Such a low value was obtained because the presence of two polymerization loci contributes in increasing the PDI, and reduces the value of k_{tp} required to obtain a given PDI. Finally, the "simultaneous polymerization" model did not capture the long high-molecular-weight tails on the experimental MWDs.

Although no calculations have been carried out, the current model should be able to account for the decreasing bimodality of the MWD with increasing temperature, as observed experimentally (Saraf et al., 2002a). The increase of temperature has little effect on the intrinsic termination rate constant of radical combination reactions because of the very low activation energy of these reactions (Matyjaszewski and Davis, 2002). On the other hand, the diffusion coefficients of the macroradicals should increase with temperature. This will cause kinetically controlled termination to extend to a higher chain length (i.e. n_{cr} will shift to a higher value as temperature increases). Consequently, the population of the unhindered radicals will increase at the expense of the hindered radicals, which in turn will result in a decrease in the bimodality.

The current model including the CTP reaction is a major improvement over the original model (Ahmed et al., 2004), especially for predicting the PDI, and the existence and behavior of bimodality. Nevertheless, the present model still has some deficiencies, which fall into two categories. The first is drawbacks generated from some of the model assumptions. The most prominent example is that the low-molecular-weight peak is unrealistically sharp when its maximum is located beyond n_{cr}. This sharp change reflects the assumption of a large step decrease in the termination rate constant when the radicals reach the critical length, rather than a gradual decrease with chain length, which is physically more reasonable but much more difficult mathematically. This is one of the costs of the simple approximation of the decrease in the termination rate constant with chain length.

The second category of drawbacks is the unsatisfactory prediction of some of the experimental observations. This includes underestimating the location of the peaks and hence the average molecular weights, as shown by the parity plot in Fig. 7. Only the number-average molecular weights are shown in

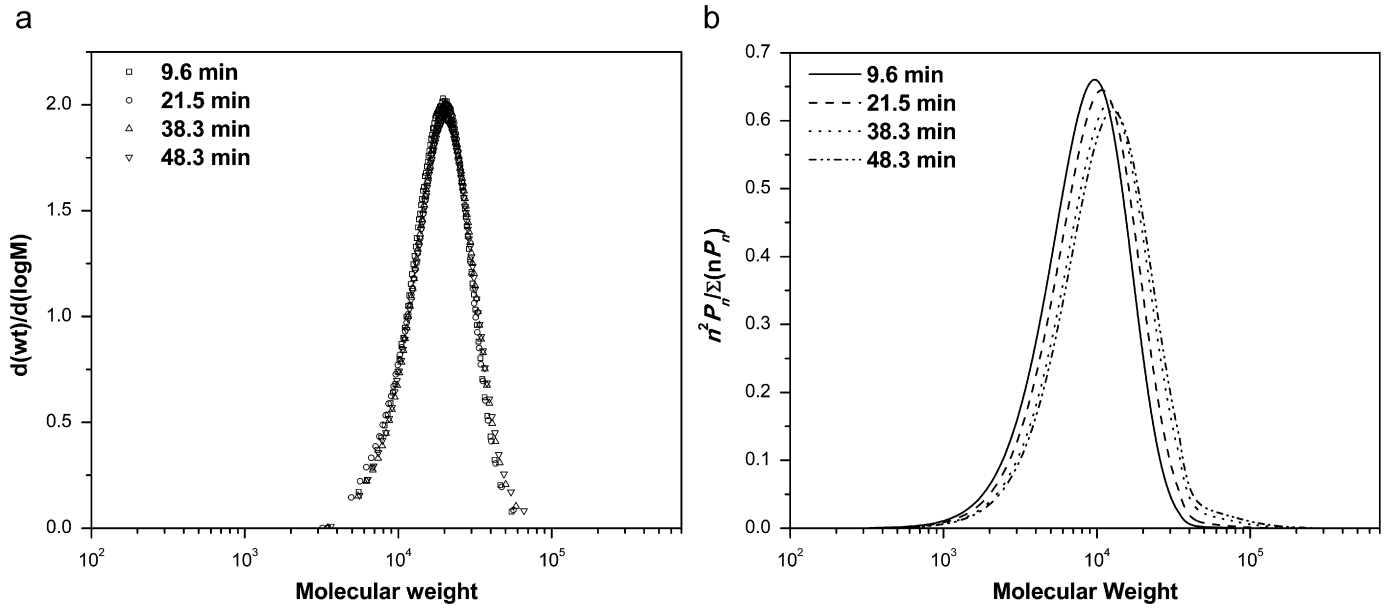

Fig. 4. Effect of average residence time on the MWD for low monomer feed concentration with M_{in}=0.78 M: (a) experimental (Saraf et al., 2002a); (b) model: the *y*-axis is proportional to the experimental one. 75 °C, 276 bar, and I_{in}=0.03 M.

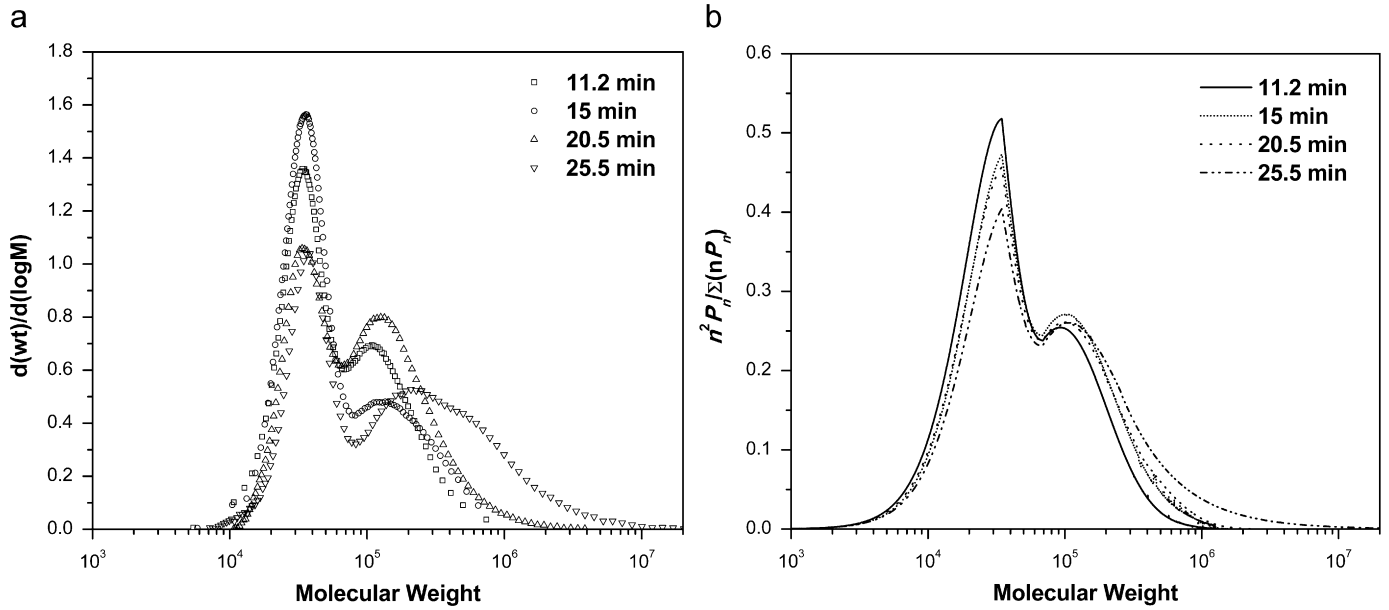

Fig. 5. Effect of average residence time on the MWD for high monomer feed concentration with M_{in}=2.8 M: (a) experimental (Saraf et al., 2002a); (b) model: the *y*-axis is proportional to the experimental one. 75 °C, 276 bar, and I_{in}=0.03 M.

this figure because the PDIs, the ratio of weight-average to number-average molecular weight, are reasonably accurate.

Saraf et al.'s (2002a) homogeneous model that contained the CTP reaction but did not account for the variation of k_t with chain length also underestimated the molecular weights of the PVDF. They attributed this to one of the two possibilities. The first was uncertainty in the value of the DEPDC initiator efficiency (Saraf et al., 2002a) reported by Charpentier et al. (2000b).This value was obtained for the reaction between ethoxy radicals and galvinoxyl radicals in the presence of CO_2 only. The efficiency of the reaction between ethoxy radicals and VF2 monomer in the presence of CO_2, VF2, and PVDF might not be the same. The second possibility is that there was a systematic error in the experimental values of the molecular weights obtained from the GPC. In fact, the number-average molecular weights obtained from nuclear magnetic resonance spectroscopy end-group analysis were lower than those measured using GPC and were closer to the model predictions (Saraf, 2001).

Uncertainty in the experimental molecular weights for PVDF also may contribute to the differences between the model and the data. For example, the experimental procedure for PVDF polymerization in $scCO_2$ involved extraction of the monomer and initiator from the synthesized polymer using $scCO_2$ after the polymer collection (Saraf et al., 2002a). This extraction might have removed some of the lowest-molecular-weight chains. Accordingly, the polymer that was analyzed with gel permeation chromatography (GPC) would show higher average molecular weights than the originally synthesized polymer. Another factor is

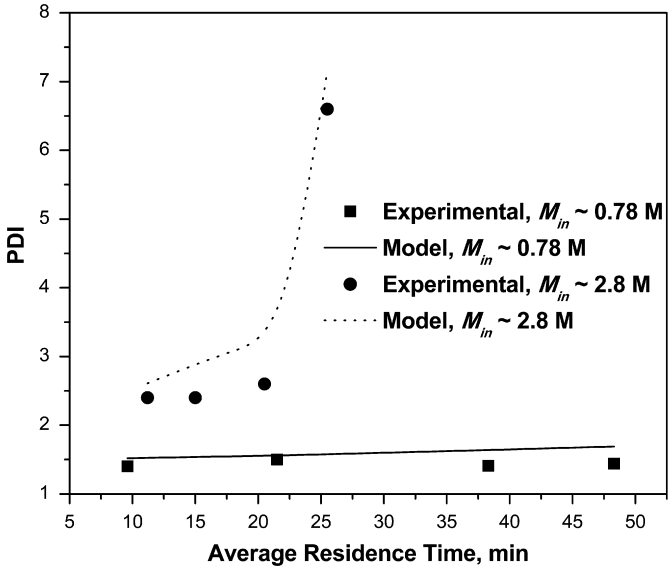

Fig. 6. Effect of average residence time on PDI. 75 °C, 276 bar, and I_{in}=0.03 M.

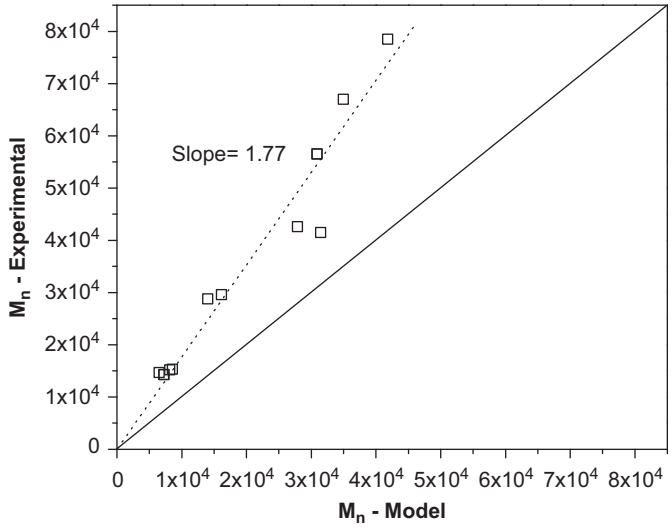

Fig. 7. Parity plot showing fit of number-average molecular weight experimental data (M_n—experimental) (GPC, against poly(methyl methacrylate)) to the number-average molecular weight predicted from the model (M_n—model). Dotted line is the best linear fit for the data points.

that the molecular weights obtained by GPC were not absolute, but were relative to poly(methyl methacrylate) standards. Moreover, these measurements were somewhat difficult (Saraf, 2001), since some PVDF samples included gelled fractions, especially at high monomer concentrations and high residence times (Scanu et al., 2005).

Finally, in the current model, the concentration of the initiator in the fluid phase was calculated with Eq. (23), which is based on the assumption that all of the initiator is in the fluid phase; i.e., there is no partitioning of the initiator between the polymer and the fluid phases. A lower concentration in the homogeneous phase as a result of partitioning should result in higher molecular weights.

In addition, among the second category of the model drawbacks, the model underestimates the size of the broad high-molecular weight peak for high monomer concentrations or high residence times. This may be due to the simplicity of the model, where only two termination reactions and rate constants have been used to approximate the hindered termination scheme that consists of an infinite number of reactions and constants. However, the uncertainty in the experimental molecular weights for PVDF also may contribute to the differences between the model and the data.

The model presented here can provide a good description of PVDF polymerization in $scCO_2$. Despite its simplicity, the model helps in understanding the origin of the bimodal MWDs observed experimentally, in predicting the polymerization behavior and the relative amount of polymer in each MWD mode, and in establishing safe control and operation for PVDF polymerizations in $scCO_2$. Finally, the hypothesis of homogeneous polymerization with two regimes of termination can be extended to interpret the experimental results of copolymerization of VF2 with hexafluoropropylene in $scCO_2$. More details are in our recent contributions (Ahmed et al., 2007, 2008, 2009).

4. Conclusions

Different hypotheses and models to account for the bimodal MWDs of PVDF synthesized in $scCO_2$ at certain conditions are reviewed. In addition, an improvement of one of these models is presented. This model is a homogeneous model that takes into account the chain transfer-to-polymer reaction, as well as the possibility that the termination reaction is either kinetically controlled or diffusion controlled, depending on the size of the participating macroradical. The diffusion-controlled termination is approximated by two reaction constants: one for the termination of unhindered and hindered radicals, and the other for termination of hindered radicals with each other.

The model can predict the occurrence of bimodal MWDs and can capture the effect of the operating parameters, e.g., the effect of monomer feed concentration and residence time on the MWD. In addition, it can capture the steep increase of the PDI of the synthesized polymers at high monomer concentrations and high residence times. Thus, the model can account for the region of inoperability observed experimentally during the continuous polymerization of PVDF.

Acknowledgment

This material is based upon work supported by the STC Program of the National Science Foundation under Agreement no. CHE-9876674.

Appendix A. Supplementary materials

The algorithm used to perform model calculations is outlined in the Supplementary data. Supplementary data associated with this article can be found in the online version at doi:10.1016/j.ces.2009.08.039.

References

Ahmed, T.S., DeSimone, J.M., Roberts, G.W., 2004. Continuous precipitation polymerization of vinylidene fluoride in supercritical carbon dioxide: modeling the molecular weight distribution. Chemical Engineering Science 59 5139–5144

Ahmed, T.S., DeSimone, J.M., Roberts, G.W., 2007. Continuous copolymerization of vinylidene fluoride with hexafluoropropylene in supercritical carbon dioxide: low hexafluoropropylene-content copolymers. Macromolecules 40, 9322–9331.

Ahmed, T.S., DeSimone, J.M., Roberts, G.W., 2008. Continuous copolymerization of vinylidene fluoride with hexafluoropropylene in supercritical carbon dioxide: high hexafluoropropylene-content amorphous copolymers. Macromolecules 41, 3086–3097.

Ahmed, T.S., DeSimone, J.M., Roberts, G.W., 2009. Kinetics of the homopolymerization of vinylidene fluoride and its copolymerization with hexafluoropropylene in supercritical carbon dioxide: the locus of polymerization. Macromolecules 42, 148–155.

Benson, S.W., North, A.M., 1959. A simple dilatometric method of determining the rate constants of chain reactions. 2. The effect of viscosity on the rate constants of polymerization reactions. Journal of the American Chemical Society 81, 1339–1345.

Bogunjoko, J.S.T., Brooks, B.W., 1983. Molecular weight distributions of poly(methyl methacrylate) produced at high viscosities. Makromolekulare Chemie—Macromolecular Chemistry and Physics 184, 1623–1643.

Buback, M., Kuchta, F.D., 1997. Termination kinetics of free-radical polymerization of styrene over an extended temperature and pressure range. Macromolecular Chemistry and Physics 198, 1455–1480.

Charpentier, P.A., DeSimone, J.M., Roberts, G.W., 2000a. Continuous precipitation polymerization of vinylidene fluoride in supercritical carbon dioxide: modeling the rate of polymerization. Industrial & Engineering Chemistry Research 39, 4588–4596.

Charpentier, P.A., DeSimone, J.M., Roberts, G.W., 2000b. Decomposition of polymerisation initiators in supercritical CO_2: a novel approach to reaction kinetics using a CSTR. Chemical Engineering Science 55, 5341–5349.

Charpentier, P.A., Kennedy, K.A., DeSimone, J.M., Roberts, G.W., 1999. Continuous polymerizations in supercritical carbon dioxide: chain-growth precipitation polymerizations. Macromolecules Communications 32, 5973–5975.

de Kock, J.B.L., Van Herk, A.M., German, A.L., 2001. Bimolecular free-radical termination at low conversion. Journal of Macromolecular Science, Polymer Reviews C41, 199–252.

Deady, M., Mau, A.W.H., Moad, G., Spurling, T.H., 1993. Evaluation of the kinetic parameters for styrene polymerization and their chain length dependence by kinetic simulation and pulsed laser photolysis. Makromolekulare Chemie 194, 1691–1705.

Dotson, N.A., Galvan, R., Laurence, R.L., Tirrell, M., 1996. Polymerization Process Modeling. VCH Publishers, New York.

Galia, A., Caputo, G., Spadaro, G., Filardo, G., 2002. γ-Radiation-initiated polymerization of vinylidene fluoride in dense carbon dioxide. Industrial & Engineering Chemistry Research 41, 5934–5940.

Galia, A., Cipollina, A., Scialdone, O., Filardo, G., 2008. Investigation of multicomponent sorption in polymers from fluid mixtures at supercritical conditions: the case of the carbon dioxide/vinylidenefluoride/poly(vinylidenefluoride) system. Macromolecules 41, 1521–1530.

Galia, A., Giaconia, A., Scialdone, O., Apostolo, M., Filardo, G., 2006. Polymerization of vinylidene fluoride with perfluoropolyether surfactants in supercritical carbon dioxide as a dispersing medium. Journal of Polymer Science, Part A: Polymer Chemistry 44, 2406–2418.

Kennedy, K.A., 2003. Characterization of Phase Equilibrium Associated with Heterogeneous Polymerizations in Supercritical Carbon Dioxide. Ph. D. thesis, Department of Chemical Engineering, North Carolina State University, Raleigh.

Klinge, U., Klosterhalfen, B., Öttinger, A.P., Junge, K., Schumpelick, V., 2002. PVDF as a new polymer for the construction of surgical meshes. Biomaterials 23 3487–3493

Liu, J., Tai, H., Howdle, S.M., 2005. Precipitation polymerisation of vinylidene fluoride in supercritical CO_2 and real-time calorimetric monitoring. Polymer 46, 1467–1472.

Lovinger, A.J., 1982. Poly(vinylidene fluoride). In: Basset, D.C. (Ed.), Developments in Crystalline Polymers. Applied Science Publishers, London, pp. 195–273.

Maccone, J., Apostolo, M., Ajroldi, G., 2000. Molecular weight distribution of fluorinated polymers with long chain branching. Macromolecules 33 1656–1663

Mahabadi, H.K., O'Driscoll, K.F., 1977. Absolute rate constants in free-radical polymerization. Part II. Termination rate constant in free-radical polymerization. Journal of Polymer Science, Polymer Chemistry Edition 15, 283–300.

Matyjaszewski, K., Davis, T.P. (Eds.), 2002. Handbook of Radical Polymerization. Wiley-Interscience, New York.

McHugh, M.A., Krukonis, V.J., 1994. Supercritical Fluid Extraction: Principles and Practice, second ed Butterworth-Heinemann, Boston.

Mueller, P.A., Storti, G., Apostolo, M., Martin, R., Morbidelli, M., 2005a. Modeling of vinylidene fluoride heterogeneous polymerization in supercritical carbon dioxide. Macromolecules 38, 7150–7163.

Mueller, P.A., Storti, G., Morbidelli, M., 2004. The reaction locus in supercritical carbon dioxide dispersion polymerization. The case of poly(methyl methacrylate). Chemical Engineering Science 60, 377–397.

Mueller, P.A., Storti, G., Morbidelli, M., 2005b. Detailed modelling of MMA dispersion polymerization in supercritical carbon dioxide. Chemical Engineering Science 60, 1911–1925.

Mueller, P.A., Storti, G., Morbidelli, M., Costa, I., Galia, A., Scialdone, O., Filardo, G., 2006. Dispersion polymerization of vinylidene fluoride in supercritical carbon dioxide. Macromolecules 39, 6483–6488.

Odian, G., 2004. Principles of Polymerization, fourth ed Wiley, New York.

Riazi, M.R., Whitson, C.H., 1993. Estimating diffusion coefficients of dense fluids. Industrial & Engineering Chemistry Research 32, 3081–3088.

Russell, G.T., 1994. On exact and approximate methods of calculating an overall termination rate coefficient from chain length dependent termination rate coefficients. Macromolecular Theory and Simulations 3, 439–468.

Russell, G.T., 1995. The kinetics of free radical polymerizing systems at low conversion. 1. On the rate determining step of the bimolecular termination reaction. Macromolecular Theory and Simulations 4, 497–517.

Saraf, M.K., 2001. Polymerization of vinylidene fluoride in supercritical carbon dioxide: molecular weight distribution. M.S. Thesis in Chemical Engineering, North Carolina State University, Raleigh.

Saraf, M.K., Gerard, S., Wojcinski, L.M., Charpentier, P.A., DeSimone, J.M., Roberts, G.W., 2002a. Continuous precipitation polymerization of vinylidene fluoride in supercritical carbon dioxide: formation of polymers with bimodal molecular weight distributions. Macromolecules 35, 7976–7985.

Saraf, M.K., Wojcinski, L.M., Kennedy, K.A., Gerard, S., Charpentier, P.A., DeSimone, J.M., Roberts, G.W., 2002b. Continuous precipitation polymerization of vinylidene fluoride in supercritical carbon dioxide: molecular weight distribution. Macromolecular Symposia 182, 119–129.

Scanu, L.F., DeSimone, J., Roberts, G.W., Khan, S.A., 2005. Is supercritical CO_2-polymerized poly(vinylidene fluoride) branched? A rheological view point. Abstracts of Papers, 229th ACS National Meeting, San Diego, CA, United States, March 13–17, 2005, PMSE-376.

Scheirs, J., 1997. Modern Fluoropolymers: High Performance Polymers for Diverse Applications. Wiley, New York.

Tai, H., Liu, J., Howdle, S.M., 2005a. Polymerisation of vinylidene fluoride in supercritical carbon dioxide: formation of PVDF macroporous beads. European Polymer Journal 41, 2544–2551.

Tai, H., Wang, W., Howdle, S.M., 2005b. Dispersion polymerization of vinylidene fluoride in supercritical carbon dioxide using a fluorinated graft maleic anhydride copolymer stabilizer. Macromolecules 38, 1542–1545.

Tai, H., Wang, W., Martin, R., Liu, J., Lester, E., Licence, P., Woods, H.M., Howdle, S.M., 2005c. Polymerization of vinylidene fluoride in supercritical carbon dioxide: effects of poly(dimethylsiloxane) macromonomer on molecular weight and morphology of poly(vinylidene fluoride). Macromolecules 38, 355–363.

Tervoort, T., Visjager, J., Graf, B., Smith, P., 2000. Melt-processable poly(tetrafluoroethylene). Macromolecules 33, 6460–6465.

Tobita, H., 1993. Molecular weight distribution in free radical polymerization with long-chain branching. Journal of Polymer Science, Part B: Polymer Physics 31, 1363–1371.

Zhang, S.X., Ray, W.H., 1997. Modeling of imperfect mixing and its effects on polymer properties. A.I.Ch.E. Journal 43, 1265–1277.